AMERICAN SOCIETY FOR MICROBIOLOGY | Journal of Virology®

VIRUS-CELL INTERACTIONS

Race against Time between the Virus and Host: Actin-Assisted Rapid Biogenesis of Replication Organelles is Used by TBSV to Limit the Recruitment of Cellular Restriction Factors

Melissa Molho,[a] Shifeng Zhu,[a] Peter D. Nagy[a]

[a]Department of Plant Pathology, University of Kentucky, Lexington, Kentucky, USA

ABSTRACT Positive-strand RNA viruses build large viral replication organelles (VROs) with the help of coopted host factors. Previous works on tomato bushy stunt virus (TBSV) showed that the p33 replication protein subverts the actin cytoskeleton by sequestering the actin depolymerization factor, cofilin, to reduce actin filament disassembly and stabilize the actin filaments. Then, TBSV utilizes the stable actin filaments as "trafficking highways" to deliver proviral host factors into the protective VROs. In this work, we show that the cellular intrinsic restriction factors (CIRFs) also use the actin network to reach VROs and inhibit viral replication. Disruption of the actin filaments by expression of the *Legionella* RavK protease inhibited the recruitment of plant CIRFs, including the CypA-like Roc1 and Roc2 cyclophilins, and the antiviral DDX17-like RH30 DEAD box helicase into VROs. Conversely, temperature-sensitive actin and cofilin mutant yeasts with stabilized actin filaments reduced the levels of copurified CIRFs, including cyclophilins Cpr1, CypA, Cyp40-like Cpr7, cochaperones Sgt2, the Hop-like Sti1, and the RH30 helicase in viral replicase preparations. Dependence of the recruitment of both proviral and antiviral host factors into VROs on the actin network suggests that there is a race going on between TBSV and its host to exploit the actin network and ultimately to gain the upper hand during infection. We propose that, in the highly susceptible plants, tombusviruses efficiently subvert the actin network for rapid delivery of proviral host factors into VROs and ultimately overcome host restriction factors via winning the recruitment race and overwhelming cellular defenses.

IMPORTANCE Replication of positive-strand RNA viruses is affected by the recruitment of host components, which provide either proviral or antiviral functions during virus invasion of infected cells. The delivery of these host factors into the viral replication organelles (VROs), which represent the sites of viral RNA replication, depends on the cellular actin network. Using TBSV, we uncover a race between the virus and its host with the actin network as the central player. We find that in susceptible plants, tombusviruses exploit the actin network for rapid delivery of proviral host factors into VROs and ultimately overcome host restriction factors. In summary, this work demonstrates that the actin network plays a major role in determining the outcome of viral infections in plants.

KEYWORDS DEAD box RNA helicase, cochaperone, cyclophilin, host factor, plant, replication, restriction factor, tomato bushy stunt virus, viral replicase, virus-host interaction, yeast

Positive-strand (+)RNA viruses are intracellular parasites that exploit host cellular resources to replicate inside the infected cells. (+)RNA viruses are the largest and most widespread plant viruses, causing important economic losses in crop production. However, plants have evolved strategies to restrict viral infections, including innate immunity, RNA silencing/RNA interference, translational repression, dominant viral

Editor Anne E. Simon, University of Maryland, College Park

Address correspondence to Peter D. Nagy, pdnagy2@uky.edu.

The authors declare no conflict of interest.

Received 31 January 2021
Accepted 18 April 2022

resistance, ubiquitin- and autophagy-mediated degradation, and the use of cell-intrinsic restriction factors (CIRFs) (1–11). As a counter response, RNA viruses have also evolved to suppress and manipulate the plant defenses and host cellular components to promote viral replication. The dynamics of virus-host interaction networks will help us to better understand plant resistance responses and develop better plant crops resistant to viruses (12–15).

Tomato bushy stunt virus (TBSV) has emerged as a highly suitable virus to study viral RNA replication and virus-host interactions. Translation of the 5′ overlapping open reading frames (ORFs) of the single TBSV genomic RNA (gRNA) results in two replication proteins, termed p33 and p92^{pol}. The abundant p33 RNA chaperone has multiple functions, including the recruitment of viral RNA template for replication and the assembly of the membrane-bound viral replicase complexes (VRCs) (16–21). The translational readthrough product of the p33 ORF is p92^{pol}, which is the RNA-dependent RNA polymerase (RdRp) (18, 22, 23). Both replication proteins are essential components of the tombusvirus VRCs (23–27).

A comparative pathosystem approach was used on two tombusviruses in a yeast (*Saccharomyces cerevisiae*) model host and plants to identify CIRFs (28–36). Genome- and proteome-wide studies of virus-host interactions using yeast mutant libraries and TBSV have identified 73 genes that reduce viral replication, possibly acting as CIRFs (29, 37–39). Most of these identified CIRFs have known orthologs in plants (40). Interestingly, in the protein-protein interaction network, multiple components of the actin cytoskeleton have emerged that either promote or restrict TBSV replication and affect TBSV recombination (29, 37, 41–44). During tombusvirus infection, the TBSV p33 replication protein subverts the actin cytoskeleton by sequestering the actin depolymerization factor, cofilin (ADF in plants), to reduce actin filament disassembly and stabilize the actin filaments/cables. Then, TBSV utilizes the stable actin filaments as "trafficking highways" to facilitate the recruitment of proviral host factors to build viral replication organelles (VRO) (42, 45).

We wanted to learn if the host cells might also use the actin filaments to deliver selected CIRFs into VROs to inhibit TBSV replication. We selected previously characterized TBSV restriction factors, such as cyclophilins (yeast Cpr1 and Cpr7, *Arabidopsis* Roc1 and Roc2, and human CypA) (38, 46). Cyclophilins are a highly conserved protein family with prolyl isomerase activity that catalyzes the *cis-trans* isomerization of the peptidyl-prolyl bonds and are involved in the assembly of multidomain proteins and in protein refolding after trafficking through cellular membranes, thus altering the structure, function, or localization of the so-called client proteins (47, 48). The yeast Cpr7 and Cpr1, the *Arabidopsis* AtRoc1 (Cyp18-3) and AtRoc2 (Cyp19-3), or the human ortholog CypA reduces TBSV replication by (i) inhibiting the recruitment of viral RNA by p33 replication protein, (ii) inhibiting VRC assembly, and (iii) blocking viral RNA synthesis (38, 46, 49–51).

Additional CIRFs selected for this work are the heat shock protein cochaperones (Sgt2 and Sti1), and a plant-specific host DEAD box RNA helicase (RH30). The host Cpr7, Sgt2, and Sti1 are tetratricopeptide repeat (TPR) domain-containing cellular proteins, which inhibit tombusvirus replication via binding and interfering with p33 replication protein functions (38, 46, 51–53). Interestingly, here, we found that the presence of all of the CIRFs tested was lower within the viral replication complexes in cofilin and actin temperature-sensitive mutant yeasts with stable actin filaments. This is in contrast with the more efficient recruitment of several proviral host factors into VROs in the same yeast mutants (41, 42, 54). By expressing the RavK effector of the *Legionella pneumophila* bacterium, which destroys the actin filaments, we show highly reduced recruitment of the CIRFs into VROs, demonstrating that dependence of CIRF functions on the actin network. Based on our findings, we suggest that there is a race between TBSV and the host for delivering both proviral and antiviral restriction factors via actin filaments into VROs. The stabilized actin filaments help TBSV with supporting rapid VRO assembly, while restricting the delivery of the restriction factors into VROs. Thus, the rapid speed of VRO assembly assisted by the subverted actin network is one of the

ways TBSV might outrace and ultimately overwhelm cellular defenses during infection of susceptible hosts.

RESULTS

The dynamic actin filaments play a key role in affecting the recruitment of cellular cyclophilin restriction factors into tombusvirus VROs in yeast. To study if actin network dynamics affect the delivery of host restriction factors into TBSV VRCs, we utilized temperature-sensitive (ts) *ACT1* and *COF1* mutant haploid yeast strains (55). These yeast strains form more stable actin filaments than wild-type (WT) yeast, which has dynamic actin network with actin patches (i.e., branched actin filaments) and longer filaments (56). Both act1^{ts} and cof1^{ts} yeasts support higher level of TBSV replication due to the stable actin-filament-assisted rapid VRO assembly (41, 42, 54). Yeasts were grown at permissive (23°C) and semipermissive (32°C) temperatures, and an intermediate temperature (29°C) and TBSV replicon RNA (repRNA) replication was started by coexpressing repRNA, Flag-tagged p33 and Flag-p92 replication proteins, and one of the His$_6$-tagged restriction factors. We found that His$_6$-Cpr1 was poorly copurified with the Flag-p33/Flag-p92^{pol}, representing the tombusvirus replicase (VRC) from membrane fraction of act1^{ts} or cof1^{ts} yeasts cultured at the semipermissive temperature (i.e., 32°C) compared with the WT yeast (Fig. 1A and B, lane 8 versus lane 7). However, Cpr1 was as efficiently copurified with the tombusvirus replicase from act1^{ts} yeast cultured at the permissive temperature (i.e., 23°C) as from WT yeast (Fig. 1A and B, lane 2 versus 1). Yeasts act1^{ts} or cof1^{ts} strains cultured at the intermediate temperature showed reduced levels of copurified Cpr1 in the replicase preparations but not as much as was found for the semi-permissive samples (Fig. 1A, lane 5 versus 4). We performed comparable replicase purification experiments using CypA, the mammalian ortholog of the yeast Cpr1, from act1^{ts} and cof1^{ts} yeasts (Fig. 1C and D). Interestingly, the data obtained with CypA were comparable to the above Cpr1 data, showing a greatly reduced amount of co-purified cyclophilins from yeast mutants with the stabilized actin filaments (Fig. 1E).

Copurification of the Cyp40-like His$_6$-Cpr7 with the tombusvirus replicase from act1^{ts} and cof1^{ts} yeasts cultured at the semipermissive temperature was also much lower than that from WT yeast (Fig. 2A and B). A similar picture was observed when we expressed only either the TPR^{cpr7} domain (Fig. 2C and D) or Cyp^{cpr7} domain (Fig. 2F), resulting in poor copurification with the viral replicase from act1^{ts} and cof1^{ts} yeasts cultured at the semipermissive temperature. Both domains of Cpr7 (Fig. 2E) interact with p33 and p92^{pol}, but the TPR^{cpr7} domain is the most effective restriction factor (51). Altogether, the obtained data support a model that the stabilized actin filaments in act1^{ts} and cof1^{ts} yeasts assist TBSV replication by reducing the recruitment of different cyclophilin restriction factors into TBSV VROs.

The dynamic actin filaments also affect the recruitment of other restriction factors into tombusvirus VROs in yeast. To learn whether the above findings with the host cyclophilins and the role of actin filaments might be a more general phenomenon during TBSV replication, we tested additional host CIRF factors. First, the cytoplasmic cochaperone Sgt2, which contains a TPR domain and inhibits tombusvirus replication (50), was tested. We found that His$_6$-Sgt2 and the His$_6$-TPR^{sgt2} domain were poorly copurified with the Flag-p33/Flag-p92^{pol} replicase from the membrane fraction of act1^{ts} or cof1^{ts} yeasts cultured at the semipermissive temperature in comparison with those of the WT yeast (Fig. 3A). However, His$_6$-Sgt2 and His$_6$-TPR^{sgt2} with 70 to 110% efficiency were copurified with the tombusvirus replicase from act1^{ts} or cof1^{ts} yeasts cultured at the permissive temperature as from WT yeast (Fig. 3A).

Second, the role of the dynamic actin network in recruitment of another effective CIRF against TBSV, namely, the *Arabidopsis* RH30 DEAD box helicase (52), was also tested. We observed a 70 to 80% reduced level of copurification of His$_6$-RH30 helicase with the Flag-p33/Flag-p92^{pol} replicase from the membrane fraction of act1^{ts} or cof1^{ts} yeasts cultured at the semipermissive temperature compared with that of the WT yeast (Fig. 3B). This was in contrast with the relatively efficient copurification of His$_6$-RH30 with the tombusvirus replicase from act1^{ts} or cof1^{ts} yeasts cultured at the permissive

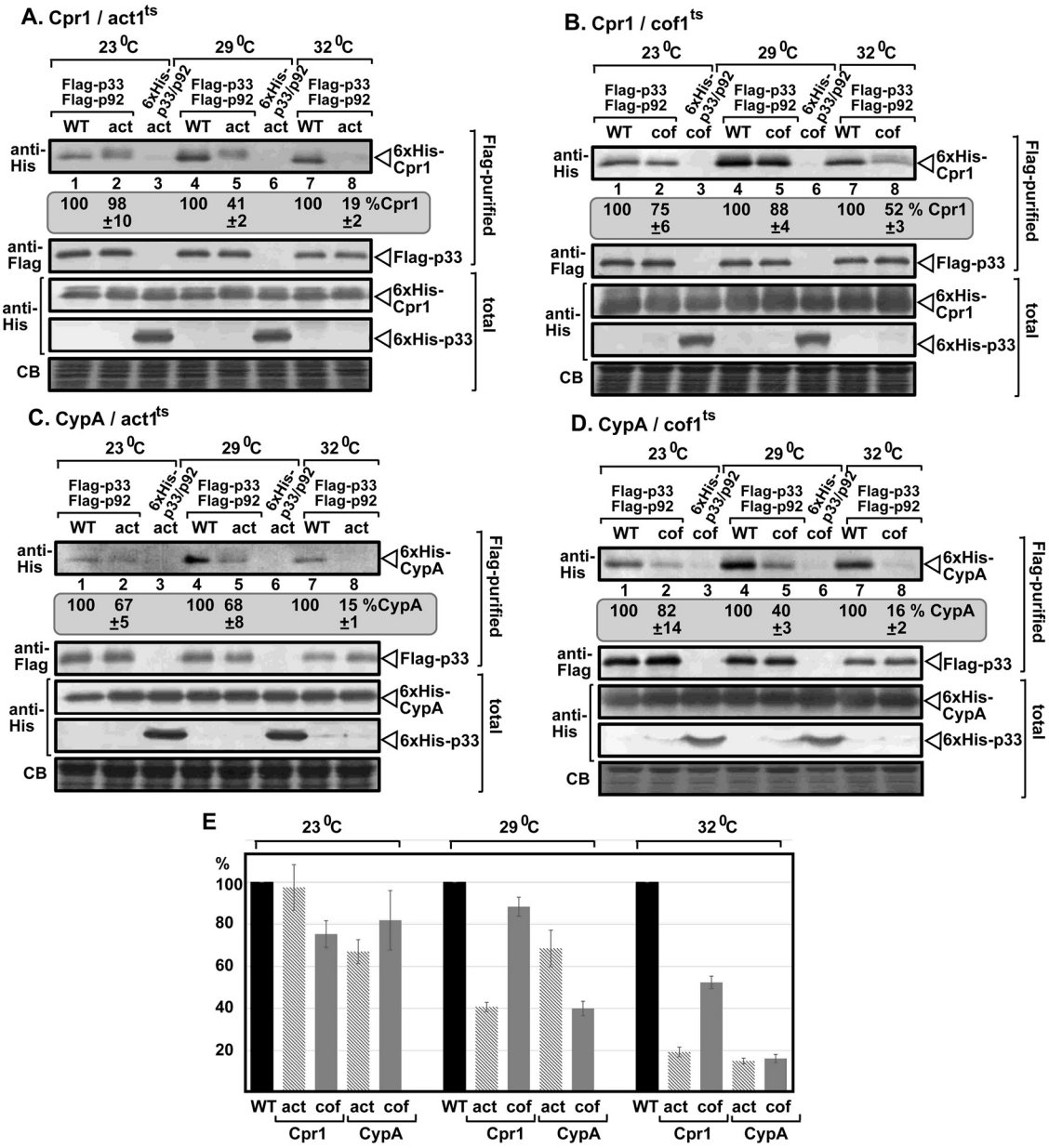

FIG 1 Temperature-sensitive actin and cofilin mutant yeasts affect the recruitment of cyclophilins into TBSV VRC. (A) The amounts of copurified yeast Cpr1 cyclophilin in the p33/p92 replicase preparations were reduced in act1-121^{ts} mutant yeast cultured at the semipermissive temperature (32°C). The Flag-tagged p33 and p92^{pol} viral replication proteins and the viral (+)repRNA together with His_6-tagged Cpr1 were expressed in WT (BY4741) and act1-121^{ts} mutant yeasts, followed by Flag affinity purification from the detergent-solubilized membrane fraction of yeasts. Expression of the His_6-tagged p33 and p92^{pol} viral replication proteins were used as a control. (Top row) Western blot analysis shows the copurified levels of His_6-Cpr1 in WT and act1-121^{ts}. Cpr1 protein was detected with anti-His antibody. (Second row) Western blot of the purified viral Flag-p33 and Flag-p92^{pol} detected with anti-FLAG antibody. (Third row) Western blot analysis of the His_6-Cpr1 levels in the total protein extracts from yeasts. (Fourth row) Western blot analysis of the His_6-p33 protein levels in the total protein extract. (Fifth row) Coomassie blue-stained SDS-PAGE of the total protein levels. (B) The copurified levels of Cpr1 were reduced in cof1-8^{ts} mutant yeasts cultured at the semipermissive temperature. See further details in panel A. (C to D) The copurified levels of CypA were reduced in actin and cofilin mutant yeasts cultured at the semipermissive temperature. Flag-p33 and Flag p92^{pol} were coexpressed with His_6-tagged CypA. See further details in panel A. (E) Each experiment was repeated three times, and the bar plot graphic represents the average levels of co-purified Cpr1 and CypA in the viral replicase preparations in WT, act1-121^{ts}, and cof1-8^{ts}. Error bars represent the standard error of the mean (SEM).

temperature (Fig. 3B). Thus, in addition to cyclophilins, a cochaperone, and an antiviral DEAD box helicase, recruitment also depends on the actin network.

To further test the role of the actin network in CIRF recruitment, we used carnation Italian ringspot virus CIRV, which is closely related to TBSV, but it replicates in a different

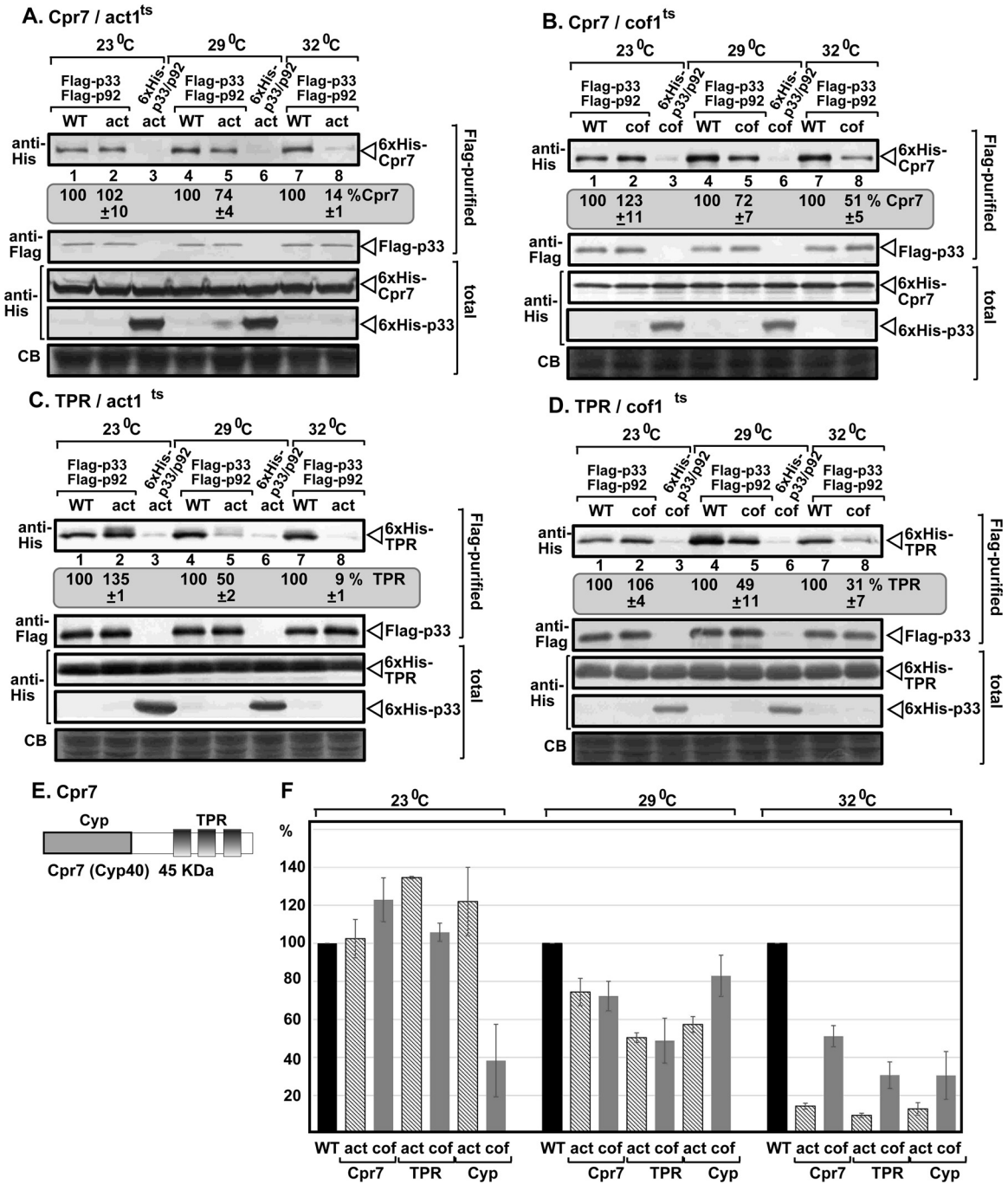

FIG 2 Temperature-sensitive actin and cofilin mutant yeasts affect the recruitment of Cyp40-like Cpr7 and its Cyp and TPR domains into TBSV VRC. (A) The amounts of copurified yeast Cpr7 cyclophilin in the p33/p92 replicase preparations were reduced in act-121^{ts} mutant yeast cultured at the semipermissive temperature (32°C). The Flag-tagged p33 and p92^{pol} viral replication proteins and the viral (+)repRNA together with His$_6$-tagged Cpr7 were expressed in WT (BY4741) and act1-121^{ts} mutant yeasts, followed by Flag affinity purification from the detergent-solubilized membrane fraction of yeasts. Expression of the His$_6$-tagged p33 and p92^{pol} viral replication proteins were used as a control. (Top row) Western blot analysis shows the copurified levels of His$_6$-Cpr7 in WT and act-121^{ts} yeasts detected with anti-His antibody. (Second row) Western blot of the purified viral Flag-p33 and Flag-p92^{pol} detected with anti-FLAG antibody. (Third row) Western blot analysis of the His$_6$-Cpr7 levels in the total protein extracts from yeasts. (Fourth row) Western blot analysis of the His$_6$-p33 protein levels in the total protein extract. (Fifth row) Coomassie blue-stained SDS-PAGE of the total protein levels. (B) The copurified levels of Cpr7 were reduced in cof1-8^{ts} mutant yeasts cultured at semipermissive temperature. See further details in panel A. (C to D) The copurified levels of His$_6$-TPR^{cpr7} (only the TPR domain of Cpr7 was expressed) were reduced in actin and cofilin mutant yeasts cultured at the semipermissive temperature. Flag-p33 and Flag p92^{pol} were coexpressed with His$_6$-TPR^{cpr7}. See further details in panel A. (E) The domain structure of the Cyp40-like Cpr7. (F) Each experiment was repeated three times, and the bar plot graphic represents the average levels of copurified full-length Cpr7, TPR^{cpr7}, and CYP^{cpr7}, respectively, in the viral replicase preparations in WT, act1-121^{ts}, and cof1-8^{ts}. Error bars represent the standard error.

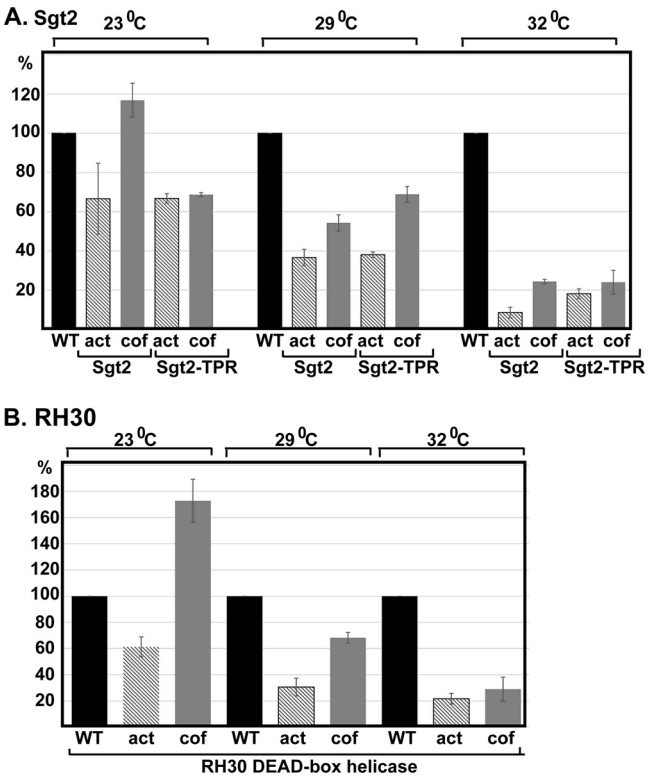

FIG 3 The recruitment of the Sgt2 cochaperone and the RH30 helicase into TBSV VRC depends on the actin network. (A and B) Graphic representation of the average levels of copurified full-length Sgt2, TPR^{sgt2}, and RH30 DEAD box helicase, respectively, in the viral replicase preparations in WT, act1-121^{ts}, and cof1-8^{ts}. The experiments were performed as described in the legend to Fig. 1. Each experiment was repeated three times. Error bars represent the standard error.

milieu, utilizing the outer surface of aggregated mitochondria (21, 57). The CIRF tested was the Hop1-like Sti1 cochaperone, which specifically restricts the replication of CIRV, but not the peroxisome-associated TBSV replication in yeast (58). We found a 60 to 70% reduction in the copurified His_6-Sti1 cochaperone with the CIRV Flag-p36/Flag-$p95^{pol}$ replicase from the membrane fraction of act1^{ts} or cof1^{ts} yeasts cultured at the semipermissive temperature compared with that of the WT yeast (Fig. 4). Conversely, the His_6-Sti1 cochaperone was efficiently copurified with the CIRV replicase from both act1^{ts} and cof1^{ts} yeasts cultured at the permissive temperature (Fig. 4C). Altogether, the emerging theme is that the stabilized actin filaments in act1^{ts} and cof1^{ts} yeasts lead to reduction of the recruitment of different CIRFs into TBSV or CIRV VROs.

For comparison, we have tested the recruitment of several proviral host factors into the tombusvirus VROs in the above yeast mutants. As expected, copurified Osh6 and Vap27-1 proteins, which are part of the virus-induced membrane contact sites (vMCS), were slightly more abundant in the TBSV Flag-p33/Flag-$p92^{pol}$ replicase preparations in cof1^{ts} yeast (Table 1) and CIRV Flag-p36/Flag-$p95^{pol}$ replicase preparations in act1^{ts} yeast cultured at the semipermissive temperature compared with those in the WT yeast (Table 2). The amounts of copurified proviral Pbp2 and Vps23 ESCRT-I protein in the TBSV and CIRV replicase preparations were comparable in cof1^{ts} or act1^{ts} yeasts cultured at the semipermissive temperature compared with those in the WT yeast (Tables 1 and 2) (42). Thus, the yeast mutants with stabilized actin filaments supported reduced recruitment of the antiviral CIRFs into VROs, whereas the same yeast mutants showed enhanced subversion of a set of proviral host factors.

Dynamic actin filaments affect the recruitment of cellular restriction factors into tombusvirus VROs in *Nicotiana benthamiana*. To study the role of the actin network in CIRF recruitment into TBSV VROs in *N. benthamiana*, we applied a new approach based on a *Legionella* bacterium effector, namely, RavK protease, which cleaves off actin monomers from the actin filaments not at the canonical position. The

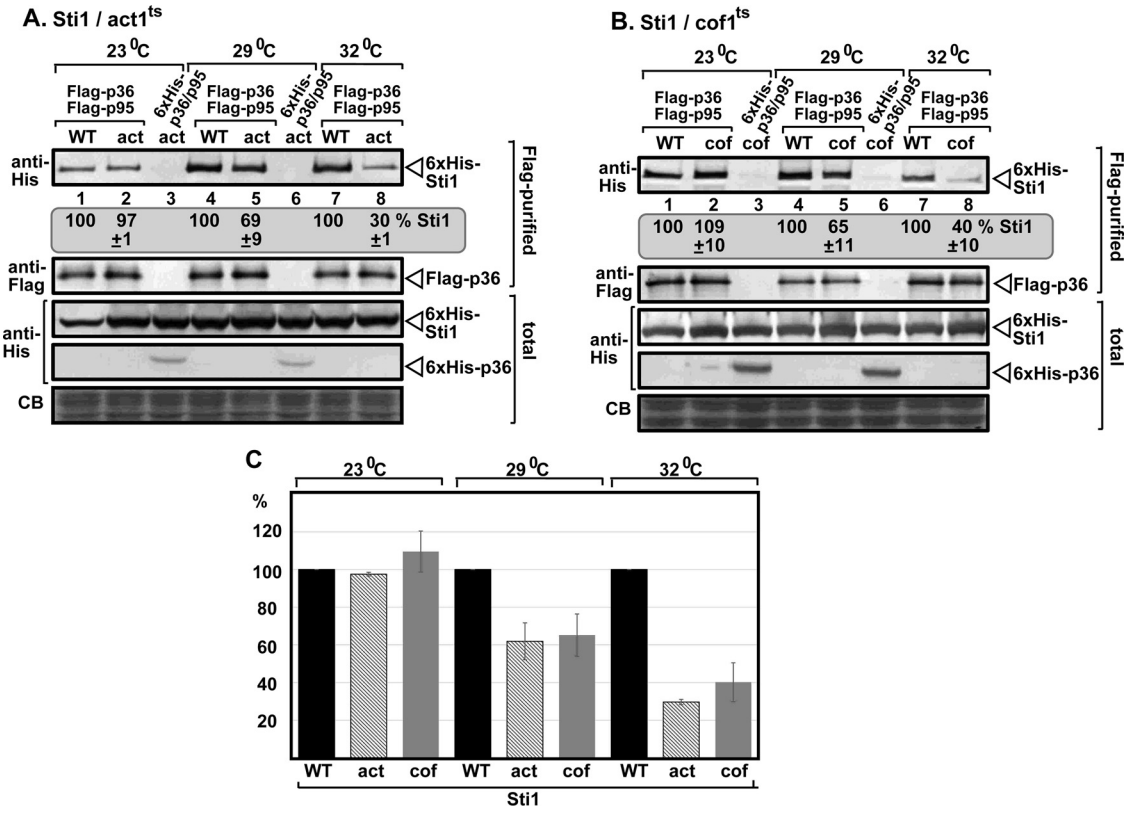

FIG 4 The recruitment of the anti-CIRV-specific Hop1-like Sti1 cochaperone into CIRV VRC depends on the actin network. (A and B) The amounts of copurified yeast Sti1 cochaperone in the CIRV p36/p95^{pol} replicase preparations were reduced in act-121^{ts} and cof1-8^{ts} mutant yeasts, respectively, cultured at the semipermissive temperature (32°C). The Flag-tagged p36 and p95^{pol} CIRV replication proteins and the viral (+)repRNA together with His_6-tagged Sti1 were expressed in WT (BY4741) and mutant yeasts, followed by Flag affinity purification from the detergent-solubilized membrane fraction of yeasts. See further details in the legend to Fig. 1. (C) Graphic representation of the average levels of copurified full-length Sti1 in the CIRV replicase preparations in WT, act1-121^{ts}, and cof1-8^{ts} yeasts. Each experiment was repeated three times. Error bars represent the standard error.

RavK activity thus leads to the destruction of most of the actin filaments in cells (59). RavK was found to inhibit TBSV replication in yeast based on a high-throughput screen (60). We found that low-level transient expression of *Legionella* RavK in *N. benthamiana* leaves infected with TBSV resulted in the formation of only small VROs decorated with p33-BFP and RFP-SKL (peroxisomal luminal marker) (Fig. 5A). This is in contrast with the characteristic large TBSV VROs consisting of aggregated peroxisomes in the absence of RavK expression (Fig. 5A). RavK expression led to small actin patches and mostly eliminated the actin filaments in *N. benthamiana* leaves (Fig. 5B and C), whereas the actin filaments were abundant in TBSV-infected cells (Fig. 5B) (42). The combination of RavK expression and TBSV infection seems to be not enough to restore the actin filaments, suggesting that the effect of RavK is dominant over the p33-cofilin-driven stabilization of actin filaments and actin cables. Nevertheless, the p33 replication protein was still localized to the peroxisomes, which did not show extensive aggregation in TBSV-infected cells also expressing RavK (Fig. 5A and B) (61).

TABLE 1 Copurified host proteins with TBSV p33 from cof1-8 yeast (32°C)[a]

Protein	Percentage[b]
Osh6 ORP	120 ± 11
Pbp2 RNA binding	98 ± 7
Vap27-1 (Scs2-like)	122 ± 10
Vps23 ESCRT I	88 ± 7

[a]Copurification of the given host protein with p33 from WT yeast was taken as 100%.
[b]Percentage of the given host protein co-purified with p33 from WT yeast grown at the same temperature.

TABLE 2 Copurified host proteins with CIRV p36 from act1-132 yeast (32°C)[a]

Protein	Percentage[b]
Ded1 helicase	97 ± 9
Osh6 ORP	160 ± 21
Pbp2 RNA binding	95 ± 11
Vap27-1 (Scs2-like)	130 ± 13
Vps4 AAA+ ATPase	63 ± 8
Vps23 ESCRT I	110 ± 8

[a]Copurification of the given host protein with p36 from WT yeast was taken as 100%.
[b]Percentage of the given host protein co-purified with p33 from WT yeast grown at the same temperature.

To confirm the inhibitory role of RavK-based destruction of actin filaments on TBSV RNA synthesis within VROs, we used a double-stranded RNA (dsRNA) sensor, which can detect the dsRNA replication intermediates during TBSV replication in plants (52, 62). We observed poor accumulation of dsRNA within the TBSV p33-BFP and RFP-SKL-decorated TBSV VROs in *N. benthamiana* leaves expressing RavK (Fig. 6A). This is in contrast with the high accumulation of TBSV dsRNA within VROs in control plants (Fig. 6A, bottom). In addition, we also utilized a modified (+)repRNA carrying an single-stranded RNA (ssRNA) sensor (21). This ssRNA sensor consists of six repeats of a hairpin RNA from MS2 bacteriophage, which is specifically recognized by the MS2 coat protein (MS2-CP) (52, 63, 64). Coexpression of the TBSV p33-BFP with RavK and the RFP-tagged MS2-CP revealed the inefficient production of the new (+)repRNA product within the active VROs (Fig. 6B, top). In the control experiments, in the absence of RavK expression, abundant new (+)repRNA product within the active VROs were detected (Fig. 6B, middle). In the presence of only the TBSV repRNA and p33-BFP (no replication due to

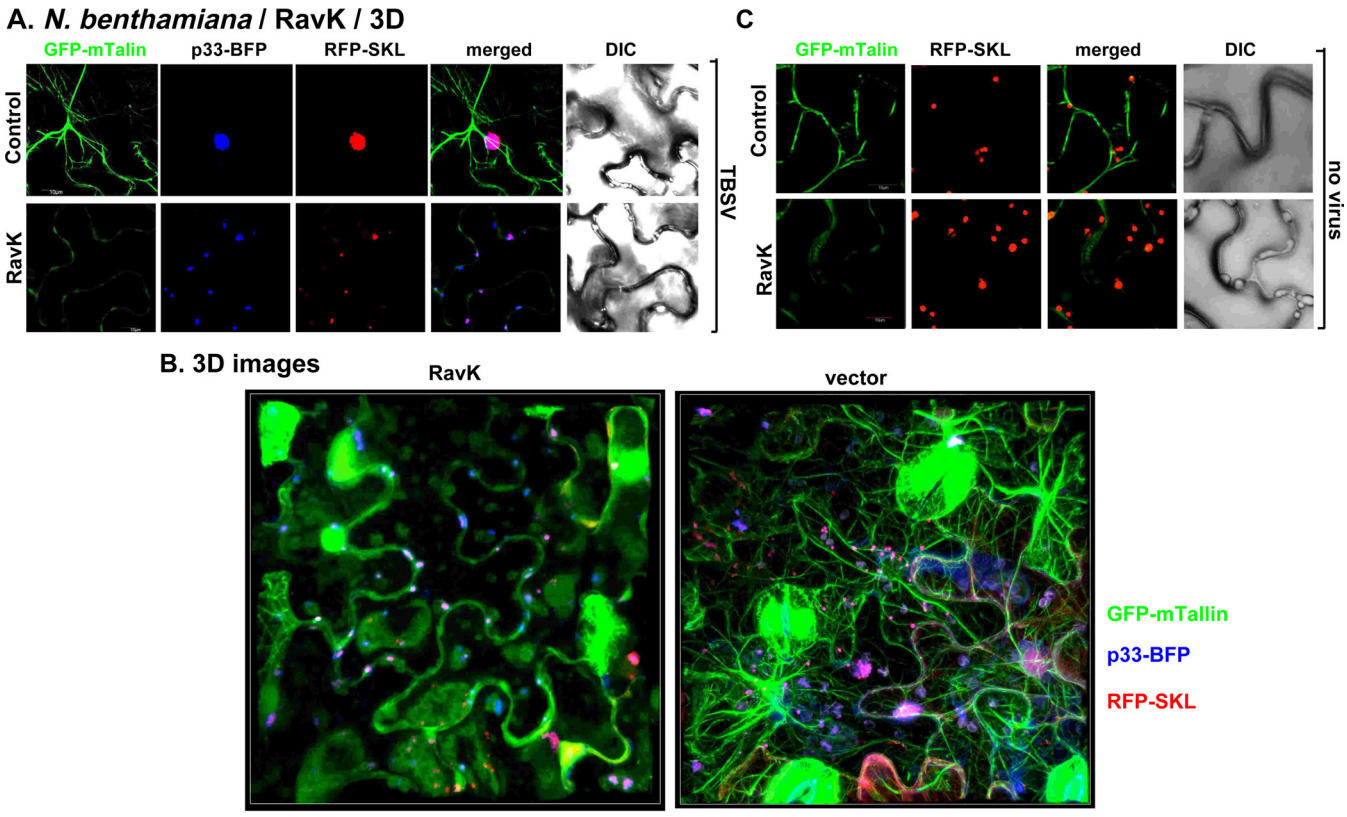

FIG 5 Transient expression of the *Legionella* RavK effector affects the architecture of the actin network and TBSV VROs in GFP-mTalin *N. benthamiana* transgenic plants. (A, top row) Transgenic *N. benthamiana* plants expressing GFP-mTalin actin-binding protein and coexpressing p33-BFP and RFP-SKL peroxisomal luminal marker (to visualize TBSV VROs). (Second row) GFP-mTalin *N. benthamiana* plants expressing p33-BFP, RFP-SKL, and the RavK effector were visualized via confocal microscopy. The plants were infected with TBSV. All of the plants were inoculated with TBSV 16 h after agroinfiltration. Plant samples were analyzed using confocal microscopy 36 h postinfection. (B) Merged three-dimensional (3D) image of plant leaves expressing the tagged-proteins as shown. See details in panel A. (C) Control transgenic *N. benthamiana* plants expressing GFP-mTalin and coexpressing RFP-SKL without (top) or with (bottom) expressing RavK effector. The plants were mock-inoculated. The scale bar is 10 μm.

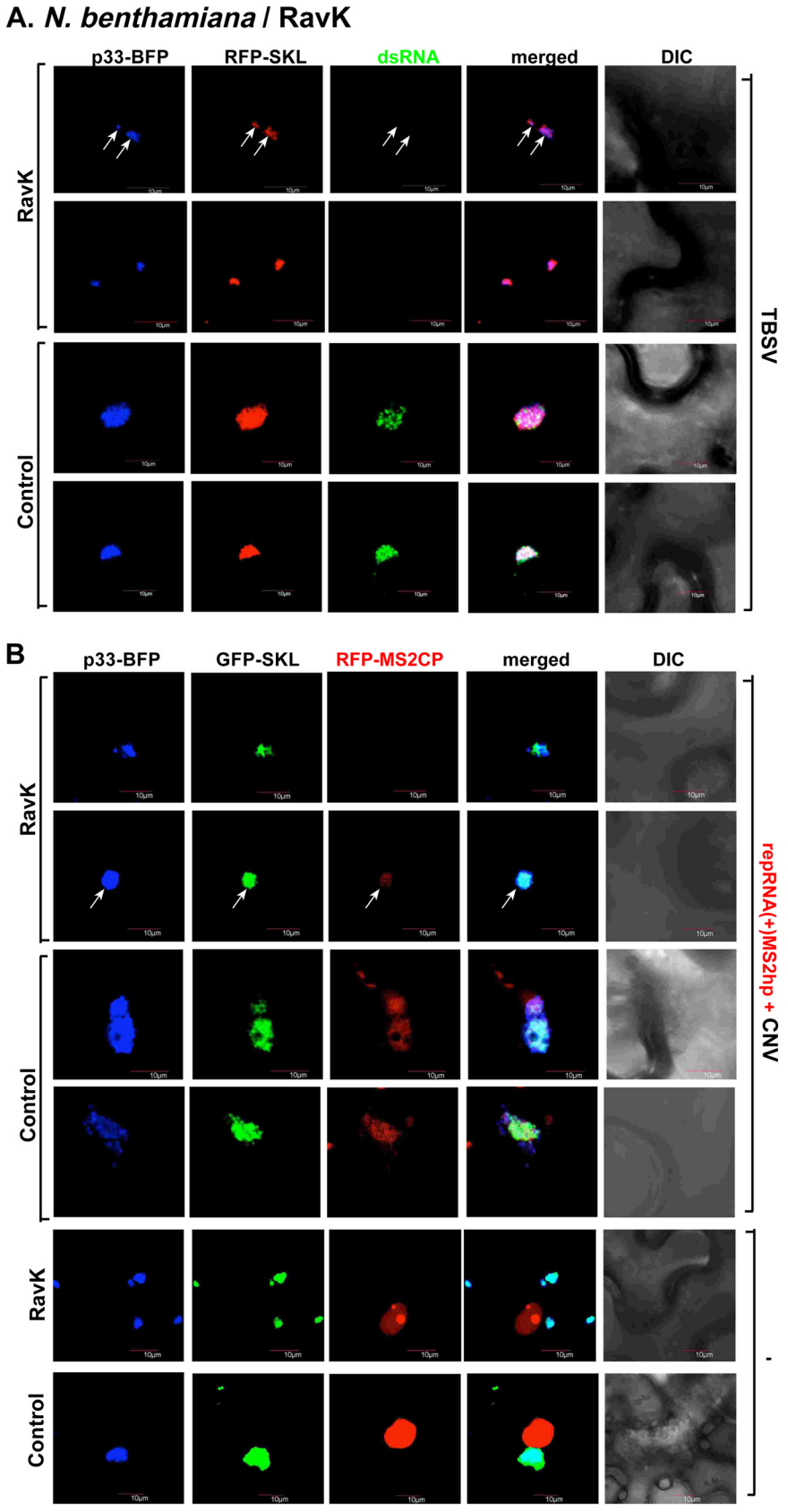

FIG 6 Transient expression of the *Legionella* RavK effector inhibits the production of dsRNA replication intermediate and (+)ssRNA progeny in TBSV VROs in *N. benthamiana* plants. (A) Reduced

(Continued on next page)

the absence of the closely related cucumber necrosis virus (CNV) helper infection), the RFP-MS2-CP was located in the nucleus with or without RavK expression (Fig. 6B, bottom). Therefore, we conclude that disruption of actin filaments by RavK greatly inhibits tombusvirus replication. In summary, the plant-based experiments confirmed that the actin filaments play an important role in tombusvirus replication. We suggest that RavK expression inhibits TBSV VRO formation via destruction of the actin filaments.

Based on the above results, we tested how the actin dynamics affect the recruitment of the CIRFs into VROs in plants. To do so, we performed a bimolecular fluorescence complementation (BiFC) assay in *N. benthamiana* leaves transiently expressing the RavK actin-cleavage effector. In addition, we also coexpressed AtRoc1 (Cyp18-3) or AtRoc2 (Cyp19-3) cyclophilins, which are plant orthologs of the yeast Cpr1 (65–67), in *N. benthamiana* leaves together with TBSV p33 replication protein. The plants were infected with TBSV. The BiFC assay data showed the lack of interaction between p33 replication protein and AtRoc1 or AtRoc2 cyclophilin proteins within VROs marked by RFP-SKL peroxisomal marker in *N. benthamiana* leaves transiently expressing RavK (Fig. 7A and C). This is in contrast with the strong interaction between p33 replication protein and either AtRoc1 or AtRoc2 cyclophilin proteins within VROs in the control *N. benthamiana* leaves not expressing RavK (Fig. 7A and C). Additional control experiments showed that the peroxisomes are not affected by RavK expression in plants (Fig. 7B and D), which indicates that RavK is not affecting protein translation under the conditions used.

Next, we confirmed the above findings using CIRV replication proteins. We found, via BiFC assay, the lack of interaction between the CIRV p36 replication protein and AtRoc1 or AtRoc2 cyclophilin proteins within VROs marked by RFP-Tim21 mitochondrial marker in *N. benthamiana* leaves transiently expressing RavK (Fig. 7E and F). As was the case with TBSV, we also observed strong interaction between the CIRV p36 replication protein and either AtRoc1 or AtRoc2 cyclophilin proteins within VROs in the control *N. benthamiana* leaves not expressing RavK (Fig. 7E and F).

Finally, we extended our BiFC analysis for the RH30 DEAD box helicase, which is a strong cytosolic restriction factor against TBSV and CIRV (52, 53). Whereas BiFC assays revealed a strong interaction between AtRH30 and TBSV p33 (Fig. 8A) or CIRV p36 replication proteins (Fig. 8C) within VROs, coexpression of RavK strongly inhibited the interaction between RH30 and TBSV p33 or CIRV p36 replication proteins (Fig. 8A and C; see also Fig. 8B for BiFC assay-negative controls). Altogether, these data suggest that disruption of the actin filaments by RavK effector inhibits the actin network-based delivery of cyclophilins and DEAD box helicase restriction factors into TBSV and CIRV VROs. The lack of the protein-protein interaction between the plant CIRFs Roc1, Roc2, and RH30 and TBSV p33 and CIRV p36 replication proteins when RavK is coexpressed is likely due to physical separation of these proteins in plant cells.

Stabilized actin filaments reduce the recruitment of cyclophilin restriction factors into tombusvirus VROs in plants. To further study the role of the actin network in CIRF recruitment into TBSV VROs in plants, we transiently expressed the *Legionella* VipA effector in *N. benthamiana* leaves. VipA is a known actin nucleator,

FIG 6 Legend (Continued)
production of the viral double-stranded RNA replication intermediate in *N. benthamiana* leaves infected with TBSV and expressing RavK effector. The TBSV dsRNA was detected via a dsRNA detector assay based on dsRNA binding-dependent fluorescence complementation. (Top) Viral dsRNA is poorly visualized within the VRO, which is marked by p33-BFP and RFP-SKL. (Bottom) TBSV dsRNA is detected in VROs in the absence of RavK expression in the control samples. Expression of the above proteins from 35S promoter was done after coagroinfiltration into *N. benthamiana* leaves. RavK effector was expressed in *N. benthamiana* leaves, and 16 h later plant leaves were inoculated with TBSV. Plant samples were collected 1.5 days postinfection (dpi). Scale bars represent 10 μm. Each experiment was repeated three times. (B) Reduced production of the viral (+)RNA products in *N. benthamiana* leaves expressing TBSV repRNA carrying MS2 hairpins and the RFP-MS2CP sensor. The plants were infected with CNV and expressed RavK effector as shown. The TBSV (+)RNA was detected via an RFP-MS2CP using confocal microscopy. Bottom images show the control images of plants with or without RavK expression and in the absence of TBSV repRNA(+)MS2hp when RFP-MS2-CP is targeted to the nucleus in the absence of cytosolic targets. Scale bars represent 10 μm. Each experiment was repeated three times.

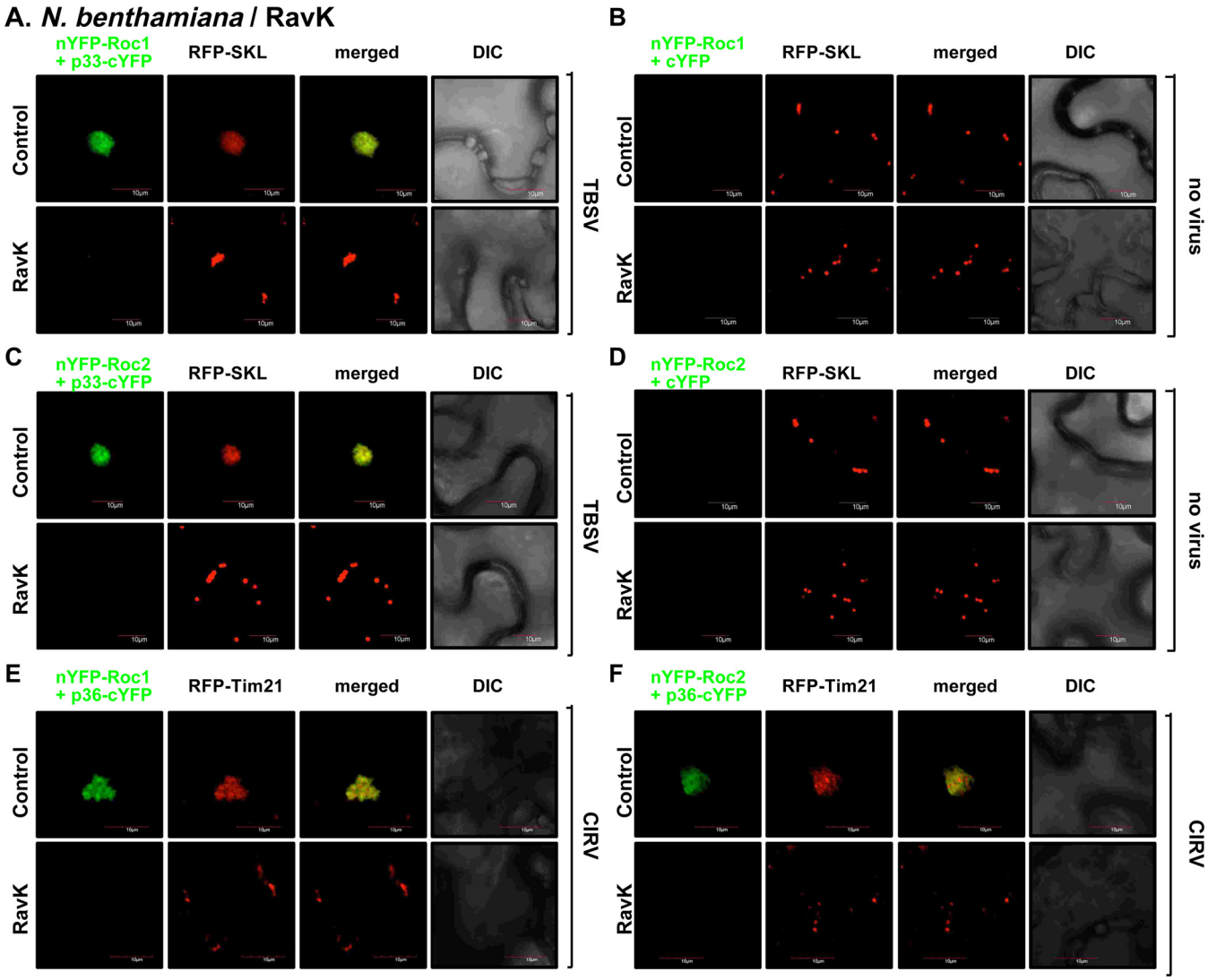

FIG 7 Disruption of the plant actin filaments by RavK expression inhibits the recruitment of plant cyclophilin restrictions factors into VROs during TBSV replication. (A, top row) Bimolecular fluorescence complementation (BiFC) analysis shows the interaction between the plant cyclophilin nYFP-Roc1 and TBSV replication protein p33-cYFP within VROs marked by RFP-SKL in control *N. benthamiana*. (Second row) On the contrary, BiFC analysis of plants also expressing RavK indicates the lack of interaction between nYFP-Roc1 and p33-cYFP within VROs. Plants were inoculated with TBSV 16 h after agroinfiltration, followed by BiFC 36 hpi. (B) Negative control experiments were performed as in panel A. (C) BiFC analysis shows the interaction between the plant cyclophilin nYFP-Roc2 and TBSV replication protein p33-cYFP within VROs marked by RFP-SKL in *N. benthamiana* not expressing and expressing RavK, respectively. Experiments were performed as in panel A. (D) Negative control experiments were performed as in panel A. (E to F) BiFC analysis shows the interaction between the plant cyclophilin nYFP-Roc1 or nYFP-Roc2 and the CIRV replication protein p36-cYFP within VROs marked by RFP-Tim21 in *N. benthamiana* not expressing and expressing RavK, respectively. Experiments were performed as in panel A, except the plant samples were visualized with confocal microscope 50 h after infection.

which promotes the formation of stable actin filaments (68), also in *N. benthamiana* (61). We have shown previously that VipA expression enhances TBSV and CIRV replication in yeast and in *N. benthamiana* (60, 61). Here, we have used BiFC assay, which showed weaker interactions between the TBSV p33 replication protein and AtRoc1 or AtRoc2 cyclophilin proteins within VROs in *N. benthamiana* leaves transiently expressing VipA (Fig. 9A and B). Compared with the control samples, we found ~2-fold less BiFC signals within VROs in cells expressing VipA (Fig. 9A and B).

The strong restriction functions of both AtRoc1 and AtRoc2 cyclophilin proteins on tombusvirus replication were mostly diminished in *N. benthamiana* leaves transiently expressing VipA (Table 3). All of these data support that the stabilized actin filaments do not favor the recruitment of these antiviral cyclophilins into tombusvirus VROs.

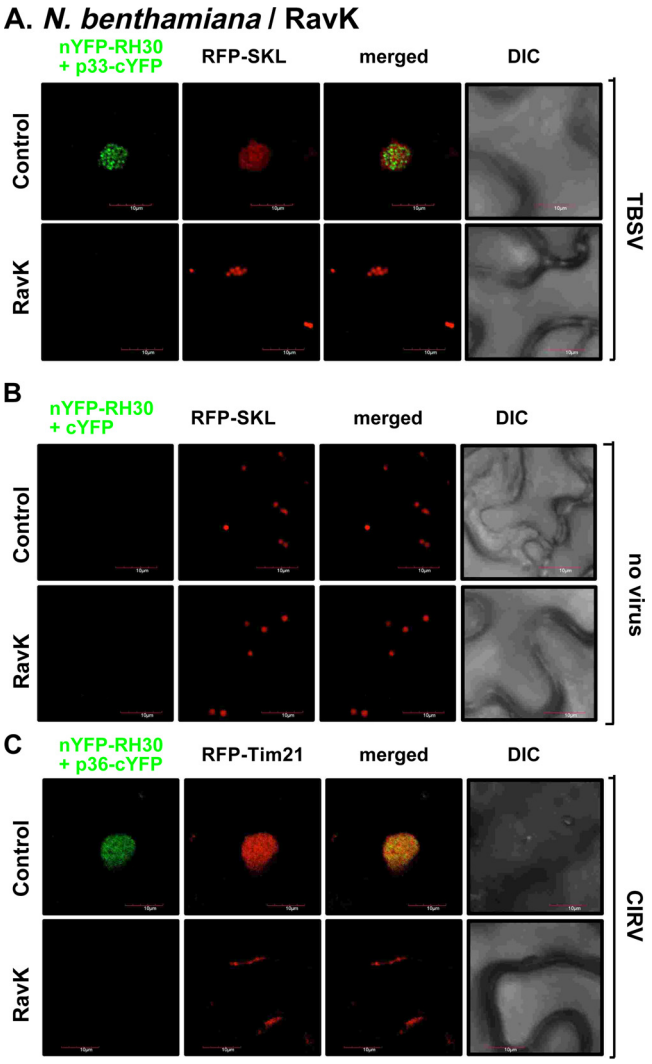

FIG 8 Inhibition of the recruitment of the antiviral RH30 DEAD box helicase into VROs via disruption of the plant actin network by RavK expression during TBSV replication. (A, top row) BiFC analysis shows the interaction between the plant nYFP-RH30 helicase and TBSV p33-cYFP replication protein within VROs marked by RFP-SKL in control *N. benthamiana*. (Second row) Comparable BiFC analysis of plants also expressing RavK indicates the lack of interaction between nYFP-RH30 and p33-cYFP within VROs. Plants were inoculated with TBSV 16 h after agroinfiltration followed by BiFC 36 hpi. (B) Negative control experiments were performed as in panel A. (C) BiFC analysis shows the interaction between the nYFP-RH30 helicase and the CIRV p36-cYFP within VROs marked by RFP-Tim21 in *N. benthamiana* not expressing and expressing RavK, respectively. Experiments were performed as in panel A, except the plant samples were visualized with confocal microscope 50 h after infection. Each experiment was repeated three times.

DISCUSSION

Tombusviruses coopt many host factors to assemble VROs for efficient virus replication (50, 69). Previous works have demonstrated that TBSV replication depends on the subversion of the actin network in infected cells. The TBSV p33 replication protein actively inhibits actin dynamics in order to efficiently recruit proviral host proteins, various lipids/membranes, and viral components to VROs, representing the replication sites (42, 54). During infection, tombusviruses remodel and stabilize the actin filaments by sequestering cofilin actin depolymerization factor (42). This leads to the stabilization of actin filaments and cables in cells. Then, TBSV utilizes the stable actin filaments to coopt proviral host factors into the rapidly forming VROs. The actin filament-assisted recruited proviral host factors include the DDX3-like Ded1 DEAD box helicase (RH20 in plants) (41), oxysterol binding proteins (OSBP-like Osh proteins), and VAP proteins

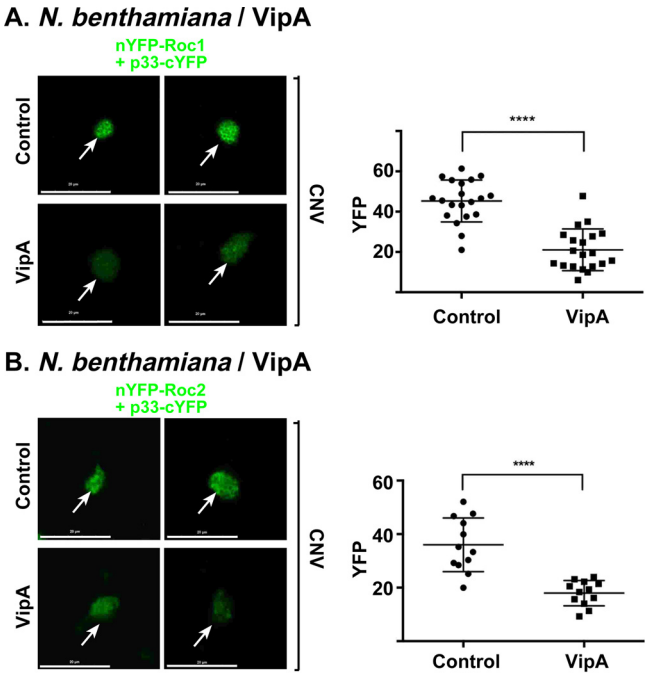

FIG 9 Inhibition of the recruitment of the antiviral CIRFs into VROs via stabilization of the plant actin filaments by VipA expression during tombusvirus replication in *N. benthamiana*. (A, top row) BiFC analysis shows the interaction between the plant nYFP-Roc1 cyclophilin and TBSV p33-cYFP replication protein within VROs in control *N. benthamiana*. (Second row) Comparable BiFC analysis of plants also expressing VipA effector indicates the reduced interaction between nYFP-Roc1 and p33-cYFP within VROs. Plants were inoculated with CNV via agroinfiltration, followed by BiFC 48 hpi. Arrows point at the VROs. The BiFC signal intensity was measured by image J. The same confocal laser microscopy setting was used in these experiments. Scale bars represent 20 μm. Each experiment was repeated three times. (B, top row) BiFC analysis shows the interaction between the plant nYFP-Roc2 cyclophilin and TBSV p33-cYFP replication protein within VROs in control *N. benthamiana*. (Second row) Comparable BiFC analysis of plants also expressing VipA effector indicates the reduced interaction between nYFP-Roc2 and p33-cYFP within VROs. See further details in panel A.

(VAMP-associated proteins) to stabilize the virus-induced membrane contact sites (vMCSs) between the endoplasmic reticulum (ER) and the peroxisome (42). The subversion of a selected group of proviral host factors into VROs was higher when the actin filaments were stable due to mutations in *ACT1* or *COF1* genes in yeast, leading to more efficient TBSV replication. Coopted proviral glycolytic and fermentation enzymes and the Rpn11 cofactor are also more efficiently recruited into tombusvirus VROs in yeast expressing the VipA effector (61).

However, the stabilized actin filaments might also facilitate the delivery of the numerous host CIRF proteins into VROs, possibly leading to inhibition of TBSV replication. Accordingly, numerous CIRFs have emerged as strong inhibitors of tombusvirus replication, raising the question of how TBSV overcomes these restrictions on viral replication (50). Indeed, in this work, we obtained evidence that the actin network plays a role in delivering CIRFs into tombusvirus VROs. We demonstrated that disruption of the actin filaments by expression of the *Legionella* RavK protease in *N. benthamiana* inhibited the recruitment of the plant CIRFs, including the CypA-like Roc1 and Roc2 cyclophilins, and the antiviral RH30 DEAD box helicase into VROs. Thus, similar to the selected group of proviral host factors, the recruitment

TABLE 3 Accumulation of CNV RNA in *N. benthamiana* expressing the shown protein(s)[a]

Empty vector	+Roc1	+VipA	+Roc1+VipA
100 ± 9	14 ± 3	233 ± 38	199 ± 31
Empty vector	**+Roc2**	**+VipA**	**+Roc2+VipA**
100 ± 11	21 ± 6	264 ± 31	221 ± 39

[a]Each experiment was repeated three times. The empty pGD vector treatment was taken as 100%.

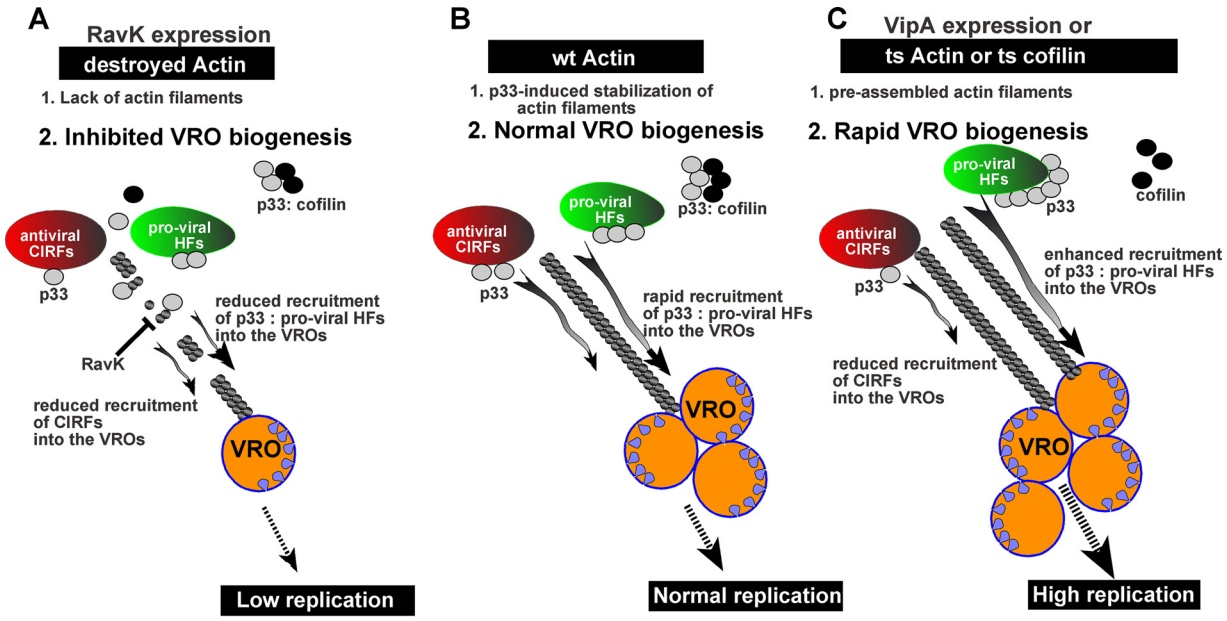

FIG 10 A model on the role of the actin network in the race to deliver restriction factors into tombusvirus VROs. (A) Disruption of the actin filaments (by RavK expression) leads to poor recruitment of both selected proviral and restriction factors into VROs. This leads to low level of replication and inhibition of VRO formation due to the unsatisfactory amounts of recruited proviral host factors. (B) During normal replication, for example in WT yeast or *N. benthamiana* plants, tombusviruses stabilize the actin filaments via sequestering cofilins with p33 replication proteins. Then, the stable actin filaments are utilized to deliver proviral host factors and also restriction factors into VROs. This is a race driven by p33 among the host factors: in these susceptible hosts, tombusviruses are capable of delivering the proviral factors more efficiently to VROs than the combined inhibitory effects provided by the recruited host restriction factors. This results in robust TBSV replication in these hosts. (C) When the host has a stabilized actin network, for example due to given mutations in actin or cofilin or expression of VipA actin nucleator, then tombusviruses easily outcompete the restriction factors via enhanced recruitment of the p33 proviral host factor complexes into VROs. Altogether, this is a race for/against VRO biogenesis between proviral and antiviral factors depending on the availability of these cellular factors and the ability of tombusviruses to subvert the host actin network in the infected hosts.

of antiviral CIRFs also depends on the existence of the dynamic actin network in cells (Fig. 10A). Dependence of the recruitment of both proviral and antiviral host factors into VROs on the actin network suggests that there is a race going on between TBSV and its host to exploit the actin network and ultimately to gain the upper hand during infection. This seems to apply to both the peroxisome-associated TBSV and the closely related mitochondria-associated CIRV. Thus, regardless of the subcellular localization of replication sites of these viruses, they depend on the actin network for VRO biogenesis.

Temperature-sensitive act1 and cofilin (cof1) mutant yeasts with stabilized actin filaments showed higher accumulation of TBSV repRNA (42). Furthermore, copurification experiments of host factors with the tombusvirus replicase suggest that TBSV is winning the race by delivering proviral host factors and viral components into VROs more efficiently than CIRFs, at least in yeast and *N. benthamiana* plants (Fig. 10A to C) (42). Accordingly, the levels of copurified CIRFs, including cyclophilins Cpr1, CypA, the Cyp40-like Cpr7, and the TPR^{Cpr7} and Cyp^{Cpr7} domains; cochaperones Sgt2, TPR^{sgt2}, and the Hop1-like Sti1; and the antiviral DDX17-like RH30 DEAD box helicase, were lower in the actin and cofilin mutant yeasts at the semipermissive temperature, which stabilizes actin filaments (55, 70). These data indicate the less efficient recruitment of antiviral host factors, when compared with the p33 replication protein, into the VROs when the actin filaments are stabilized. Similar to yeast, we also observed the reduced recruitment of the Cyp1-like Roc1 and Roc2 cyclophilins into VROs in *N. benthamiana* with stabilized actin filaments (due to expression of VipA effector) (Fig. 9). This correlates with the diminished antiviral effect Roc1 and Roc2 cyclophilins in VipA-expressing plants. It is possible that actin dynamics affect the time and/or the intracellular location available for interactions between the CIRFs and the viral replication components. It seems that more rapid assembly of the VROs with the help of stabilized actin filaments limits the recruitment of the antiviral host

factors into the VROs, thus reducing the defense response of the host against the virus. However, in hosts with a WT actin network, tombusviruses need time and have to "sacrifice" viral resources (i.e., numerous p33 molecules) to sequester the cellular cofilin actin depolymerization factor in order to stabilize the actin filaments to produce efficient VRO biogenesis (Fig. 10B). In contrast, the actin filaments are already stable in the actin and cofilin mutant yeasts at the semipermissive temperature or in *N. benthamiana* expressing the VipA effector, which actin filaments then can be readily subverted by p33 to support rapid VRO formation (Fig. 10C). The stable actin filaments also facilitate the recruitment of several proviral host factors into VROs more efficiently in the above yeast strains at the semipermissive temperature (41, 42) (see also Tables 1 and 2) or in *N. benthamiana* plants expressing the VipA effector (61). Overall, stable actin filaments favor the recruitment of several proviral factors while they disfavor the recruitment of several restriction factors into VROs. Thus, actin filament stabilizing factors shift the balance toward a more favorable cellular environment that leads to higher level of tombusvirus replication.

Ultimately, the emerging theme is that tombusviruses do not seem to have enough viral resources (i.e., enough p33 molecules per cell) to neutralize the restriction effects of all of the CIRFs produced by a given host. Therefore, the strategy of these viruses is to outrace the host restriction activities by transforming the actin network into a "racing speedway" in order to rapidly build large VROs. In turn, these VROs then protect the viral replication machinery and the viral RNA products from degradation by cellular degradative enzymes as shown before (71, 72). Thus, tombusviruses do not completely exclude CIRFs from VROs but limit their amounts and effectiveness by rapidly overloading the VROs with proviral host factors and viral components. This model explains the successful tombusvirus infections in suitable hosts, such as yeast and *N. benthamiana*. However, other hosts might have more powerful CIRF arsenals to combat tombusviruses, thus more effectively restricting tombusvirus replication and possibly even limiting the host range of tombusviruses. Thus, this work presents a key role of the actin dynamics to facilitate or restrict tombusvirus replication. Overall, the actin network and the extent of the CIRF arsenal might be major determinants of success of tombusviruses to replicate in a given host. We propose that, in highly susceptible plants, such as *N. benthamiana*, tombusviruses efficiently subvert the actin network for rapid delivery of proviral host factors and viral replication components for VRO assembly. Thus, TBSV seems to overcome host restriction factors in *N. benthamiana* via winning the race by delivering more proviral than restriction factors to the replication sites (i.e., VROs).

Multiple animal viruses also exploit the actin network to infect the host cell (73–75). Thus, to develop better and broader antiviral strategies, future research should decipher how different viruses utilize the actin network for replication, cell-cell movement, and systemic movement. The actin network is critical for the plant immune system and has become a key target for plant pathogens to subvert actin functions and infect host cells (15, 76–78). Understanding the role of the actin network in virus infection might lead to improvement of plant disease resistance against viruses and other pathogens.

MATERIALS AND METHODS

Yeast strains and expression plasmids. *Saccharomyces cerevisiae* strain BY4741 (*MAT***a** *his3*-Δ1 *leu2*-Δ0 *met15*-Δ0 *ura3*-Δ0) was obtained from Open Biosystems (Huntsville, AL, USA). To generate the plant expression plasmid pGD-2x35SL-FlagRavK, the *Legionella* RavK sequence was PCR-amplified from the lpg0969 plasmid from the *Legionella pneumophila* library (79) using primers 7664 and 7665. The PCR products were digested with BamHI and XhoI and inserted into pGD-2x35SL and pGD-2x35SL-RFP, digested with BamHI and SalI. The yeast expression plasmids pGBK-FLAGp33-CUP1/DI72-GAL1, pGBK-HISp33-CUP1/DI72-GAL1, pGAD-FLAGp92-CUP1 and pGAD-HISp92-CUP1, pYC-NT-CypA, pYES-NT-Cpr7, pYES-NT-Cpr1, and pYES-NT-RH30 have been previously described (38, 46, 51, 52, 80). To create plasmids pYES-NT-Cpr7-TPR and pYES-NT-Cpr7-Cyp, the TPR and CYP domains were PCR-amplified from the *CPR7* gene with oligonucleotide pairs of numbers 3152 plus 4132 and 4131 plus 4116, respectively, followed by digestion with BamHI and EcoRI restriction enzymes and insertion into the pYES-NT vector previously digested with BamHI and EcoRI. For yeast plasmids pYES-NT-Sti1 and pYC2-NT-Sgt2, the *STI1* gene was PCR-amplified from the yeast genomic DNA with oligonucleotide numbers 2863 and 2864, and the *SGT2* gene was PCR amplified from yeast genomic DNA with oligonucleotide numbers 4405 and 4406. Both PCR products were digested with BamHI and XhoI restriction enzymes and cloned into the pYES-NT vector digested with BamHI and XhoI. pYC2-NT-Sgt2-TPR was provided by Ching-Kai Chuang. To make the

plant expression plasmids pGDnYFP-Roc1 and pGDnYFP-Roc2, *Arabidopsis thaliana* cDNA preparation was made using primer oligonucleotide-deoxyribosylthymine (dT) and Moloney murine leukemia virus (MMLV) reverse transcriptase and 1st-strand cDNA synthesis kit (Lucigen). The *A. thaliana ROC1* and *ROC2* genes were cloned using oligonucleotides 3576 and 3492 or 3577 and 3578 for PCR amplifications. The PCR-amplified fragments were digested with BamHI and XhoI restriction enzymes and inserted into pGD-nYFP vector digested with BamHI and SalI (45).

Protein copurification assay using yeast. BY4741 (WT), act1-121^{ts}, or cof1-8^{ts} (55) yeast strains were cotransformed with pGBK-CUP-Flagp33/Gal-DI72 and pGAD-Cup-Flagp92 and one of the following plasmids: pYC-NT-CypA, pYES-NT-Cpr1, pYES-Cpr7, pYES-NT-Cpr7-TPR, pYES-NT-Cpr7-Cyp, pYES-NT-RH30, pYC-NT-Sgt2, or pYC-NT-Sgt2-TPR. The control yeasts were transformed with pGBK-CUP-Hisp33/Gal-DI72 and pGAD-Cup-Hisp92 and one of the following plasmids: pYC-NT-CypA, pYES-NT-Cpr1, pYES-Cpr7, pYES-NT-Cpr7-TPR, pYES-NT-Cpr7-Cyp, pYES-NT-RH30, pYC-NT-Sgt2, or pYC-NT-Sgt2-TPR. Because the *STI1* gene only affects CIRV replication, BY4741, act1-121^{ts}, or cof1-8^{ts} was cotransformed with pGBK-CUP-Flagp36/Gal-DI72 and pGAD-Cup-Flagp95, pYES-NT-Sti1 or HpESC-CUP-Hisp36/Gal-DI72, LpESC-Cup-Hisp95, or pYES-NT-Sti1 as a control.

The following procedure was adapted from reference 42. Briefly, selected yeast transformants were pregrown in 20 mL of SC-ULH$^-$ medium supplemented with 2% glucose and bovine calf serum (BCS) (copper chelator) for 16 h at 23°C. Then cultures were washed with water and grown in 40 mL of SC-ULH$^-$ medium supplemented with 2% galactose and BCS for 24 h at 23°C. Finally, cultures were washed and induced in SC-ULH$^-$ containing 2% galactose and 50 μM $CuSO_4$ for 6 h at 23°C, 29°C, or at 32°C. To cross-link proteins, yeast cultures were diluted in 1× phosphate-buffered saline (PBS) pH 7.4 (137 mM NaCl, 2.7 mM KCl, 10 mM Na_2HPO_4, 1.8 mM KH_2PO_4) with 1% formaldehyde and incubated on ice for 1 h. The formaldehyde was quenched with 2.5 M glycine and placed on ice for 5 min. Yeast cultures were washed with PBS buffer and stored at −80°C for further analysis.

The collected yeast pellets were resuspended in 1× volumes of high-salt TG buffer (50 mM Tris-HCl, pH 7.5; 10% glycerol; 15 mM $MgCl_2$; 10 mM KCl) with 0.1% yeast protease inhibitor (YPIC) (Sigma). Ten microliters of the yeast suspension was used to extract the total proteins based on the NaOH method (81). A total of 2.5 volumes of acid-washed glass beads were added, and the yeast cells were broken in the Fast Prep homogenizer (4 × 20 s, speed 5.5). The cells were shaken five times, and each time the tubes were placed on ice for 1 min. Yeast homogenates were centrifuged 500 × *g* for 5 min, and supernatants were transferred into new Eppendorf tubes. Then, the tubes were centrifuged at high-speed (35,000 × *g*) for 20 min, and the supernatants were discarded. The membrane fractions were solubilized with solubilization buffer (high-salt TG buffer, 2% Triton, 0.1% YPIC). Tubes were rotated for 5 h at 4°C, the solubilized yeasts were centrifuged at high-speed (35,000 × *g*) for 20 min, and supernatants were loaded onto an equilibrated Bio-Rad Bio-Spin chromatography column containing FLAG-resin (Sigma). The binding was done at 4°C for 6 h, and the columns were washed several times with high-salt TG buffer. Finally, the proteins were eluted with SDS 1× loading buffer, and the samples were collected by centrifugation 150 × *g* for 2 min; β-mercaptoethanol was added. To reverse the cross-linking, samples were boiled for 35 min. The purified and copurified proteins were analyzed by sodium dodecyl sulfate-polyacrylamide gel electrophoresis (10% SDS gels) (44). The viral protein levels were detected and normalized by Western blotting using anti-FLAG antibody, and the levels of copurified proteins were detected with the anti-His antibody. To compare the protein levels, the polyvinylidene difluoride (PVDF) membranes were scanned and quantified with ImageQuant software. The quantifications were analyzed in Excel, and standard error was calculated. Each experiment was repeated three times.

Confocal microscopy analysis and BiFC analysis in *N. benthamiana* plants. To observe the distribution of the actin filaments in plant cells during tombusvirus replication when RavK was also coexpressed, transgenic *N. benthamiana* expressing green fluorescent protein (GFP)-mTalin plants were coagroinfiltrated with pGD-2x35SL-FlagRavK (optical density at 600 nm [OD_{600}], 0.5) and pGD-p19 (OD_{600}, 0.2) or pGD-2x35SL-FlagRavK (OD_{600}, 0.5), pGD-p19 (OD_{600}, 0.2), pGD-2x35SL-cBFPp33 (OD_{600}, 0.2), and pGD-RFP-SKL (OD_{600} 0.2). Plants were also coagroinfiltrated with pGD-2x35SL vector (OD_{600}, 0.5), pGD-p19 (OD_{600}, 0.2), pGD-2x35SL-cBFPp33 (OD_{600}, 0.2), and pGD-RFP-SKL (OD_{600}, 0.2). Sixteen hours after agroinfiltration, plant leaves were inoculated with TBSV. Plant samples were visualized in the confocal laser scanning microscope (Olympus FV1000 and FV3000; Olympus America) 36 h after infection (82).

The distribution of TBSV (+)ssRNA progeny and dsRNA replication intermediate was visualized using RNA sensors expressed via agroinfiltration in *N. benthamiana* plants with a confocal laser scanning microscope as described previously (52).

For the biomolecular fluorescence complementation (BiFC) assay (83), *N. benthamiana* plant leaves were coagroinfiltrated with pGD-p33cYFP (OD_{600}, 0.2), pGD-RFP-SKL (OD_{600}, 0.2), pGD-p19 (OD_{600}, 0.15), pGD-2x35SL vector (OD_{600}, 0.5), or pGD-RFP-SKL, pGD-p33cYFP, pGD-p19, pGD-2x35SL-RavK (OD_{600}, 0.5) with one of the following plasmids: pGD-2x35SL-nYFPRoc1 (OD_{600}, 0.2), pGD-2x35SL-nYFPRoc2 (OD_{600}, 0.2), or pGD-2x35SL-nYFPRH30 (OD_{600}, 0.2), respectively. Sixteen hours after agroinfiltration, the leaves were inoculated with TBSV, and 36 h postinfection (hpi), plant leaf samples were visualized with the confocal laser scanning microscope (83). To perform BiFC during CIRV infection, pGD-p36cYFP (OD_{600}, 0.2), pGD-Tim21 (OD_{600}, 0.2), pGD-2x35SL vector (OD_{600}, 0.2), pGD-p19 (OD_{600}, 0.2), pGD-CIRV (OD_{600}, 0.2) or pGD-p36cYFP (OD_{600}, 0.2), pGD-Tim21 (OD_{600}, 0.2), pGD-CIRV (OD_{600}, 0.2), pGD-p19 (OD_{600}, 0.2), pGD-2x35SL-RavK (OD_{600}, 0.2) and one of the following vectors, pGD-nYFPRoc1 (OD_{600},0.2), pGD-nYFPRoc2 (OD_{600}, 0.2), or pGD-nYFPRH30 (OD_{600}, 0.2), were coagroinfiltrated into *N. benthamiana* plants. Samples were visualized 50 h after agroinfiltration as described above. To perform BiFC in the absence or presence of *Legionella* VipA effector, agrobacterium C58C1 containing the following respective plasmids, pGD-p33cYFP (OD_{600}, 0.3), pGD-2x35SL vector (OD_{600}, 0.3) or pGD-VipA (OD_{600}, 0.3), pGD-RFP-SKL (OD_{600}, 0.2), pGD-p19 (OD_{600}, 0.1), and pGD-CNV (20KSTOP) (OD_{600}, 0.2), and pGD-nYFP-Roc1 (OD_{600}, 0.3) or pGD-

nYFP-Roc2 (OD_{600}, 0.3) was coinfiltrated into *N. benthamiana* leaves. Samples were visualized 48 h after agroinfiltration using the FluoView FV3000 confocal laser scanning microscope (Olympus).

ACKNOWLEDGMENTS

We thank Judit Pogany for help during this work and comments on the manuscript. We thank Nikolay Kovalev for providing initial data on the copurification of proviral host factors in replicase preparations from yeast. The authors appreciate the technical contribution of R. Y. Wang to part of the work. The authors also thank Charles Boone (University of Toronto) for yeast ts mutants. Yeast expression plasmid pYC2-NT-Sgt2-TPR was provided by Ching-Kai Chuang.

This work was supported by the National Science Foundation (MCB-1517751 and IOS-1922895), USDA (NIFA, 2020-70410-32901), and a USDA hatch grant (KY012042) to P.D.N.

REFERENCES

1. Wu X, Valli A, Garcia JA, Zhou X, Cheng X. 2019. The tug-of-war between plants and viruses: great progress and many remaining questions. Viruses 11:203. https://doi.org/10.3390/v11030203.
2. Zorzatto C, Machado JP, Lopes KV, Nascimento KJ, Pereira WA, Brustolini OJ, Reis PA, Calil IP, Deguchi M, Sachetto-Martins G, Gouveia BC, Loriato VA, Silva MA, Silva FF, Santos AA, Chory J, Fontes EP. 2015. NIK1-mediated translation suppression functions as a plant antiviral immunity mechanism. Nature 520:679–682. https://doi.org/10.1038/nature14171.
3. Nicaise V. 2014. Crop immunity against viruses: outcomes and future challenges. Front Plant Sci 5:660. https://doi.org/10.3389/fpls.2014.00660.
4. Cillo F, Palukaitis P. 2014. Transgenic resistance. Adv Virus Res 90:35–146. https://doi.org/10.1016/B978-0-12-801246-8.00002-0.
5. Carr JP, Lewsey MG, Palukaitis P. 2010. Signaling in induced resistance. Adv Virus Res 76:57–121. https://doi.org/10.1016/S0065-3527(10)76003-6.
6. Truniger V, Aranda MA. 2009. Recessive resistance to plant viruses. Adv Virus Res 75:119–159. https://doi.org/10.1016/S0065-3527(09)07504-6.
7. Robaglia C, Caranta C. 2006. Translation initiation factors: a weak link in plant RNA virus infection. Trends Plant Sci 11:40–45. https://doi.org/10.1016/j.tplants.2005.11.004.
8. Ding SW. 2010. RNA-based antiviral immunity. Nat Rev Immunol 10:632–644. https://doi.org/10.1038/nri2824.
9. Li B, Meng X, Shan L, He P. 2016. Transcriptional regulation of pattern-triggered immunity in plants. Cell Host Microbe 19:641–650. https://doi.org/10.1016/j.chom.2016.04.011.
10. Ngou BPM, Ding P, Jones JD. 2022. Thirty years of resistance: zig-zag through the plant immune system. Plant Cell 34:1447–1478. https://doi.org/10.1093/plcell/koac041.
11. Yu X, Feng B, He P, Shan L. 2017. From chaos to harmony: responses and signaling upon microbial pattern recognition. Annu Rev Phytopathol 55:109–137. https://doi.org/10.1146/annurev-phyto-080516-035649.
12. Moon JY, Park JM. 2016. Cross-talk in viral defense signaling in plants. Front Microbiol 7:2068. https://doi.org/10.3389/fmicb.2016.02068.
13. Liu JZ, Li F, Liu Y. 2017. Editorial: plant immunity against viruses. Front Microbiol 8:520. https://doi.org/10.3389/fmicb.2017.00520.
14. Souza PFN, Carvalho FEL. 2019. Killing two birds with one stone: how do plant viruses break down plant defenses and manipulate cellular processes to replicate themselves? J Plant Biol 62:170–180. https://doi.org/10.1007/s12374-019-0056-8.
15. Park E, Nedo A, Caplan JL, Dinesh-Kumar SP. 2018. Plant-microbe interactions: organelles and the cytoskeleton in action. New Phytol 217:1012–1028. https://doi.org/10.1111/nph.14959.
16. Monkewich S, Lin HX, Fabian MR, Xu W, Na H, Ray D, Chernysheva OA, Nagy PD, White KA. 2005. The p92 polymerase coding region contains an internal RNA element required at an early step in tombusvirus genome replication. J Virol 79:4848–4858. https://doi.org/10.1128/JVI.79.8.4848-4858.2005.
17. Pogany J, White KA, Nagy PD. 2005. Specific binding of tombusvirus replication protein p33 to an internal replication element in the viral RNA is essential for replication. J Virol 79:4859–4869. https://doi.org/10.1128/JVI.79.8.4859-4869.2005.
18. Pogany J, Nagy PD. 2012. p33-independent activation of a truncated p92 RNA-dependent RNA polymerase of Tomato bushy stunt virus in yeast cell-free extract. J Virol 86:12025–12038. https://doi.org/10.1128/JVI.01303-12.
19. Stork J, Kovalev N, Sasvari Z, Nagy PD. 2011. RNA chaperone activity of the tombusviral p33 replication protein facilitates initiation of RNA synthesis by the viral RdRp in vitro. Virology 409:338–347. https://doi.org/10.1016/j.virol.2010.10.015.
20. Pogany J, Stork J, Li Z, Nagy PD. 2008. In vitro assembly of the Tomato bushy stunt virus replicase requires the host heat shock protein 70. Proc Natl Acad Sci U S A 105:19956–19961. https://doi.org/10.1073/pnas.0810851105.
21. Panavas T, Hawkins CM, Panaviene Z, Nagy PD. 2005. The role of the p33:p33/p92 interaction domain in RNA replication and intracellular localization of p33 and p92 proteins of Cucumber necrosis tombusvirus. Virology 338:81–95. https://doi.org/10.1016/j.virol.2005.04.025.
22. Panaviene Z, Panavas T, Nagy PD. 2005. Role of an internal and two 3'-terminal RNA elements in assembly of tombusvirus replicase. J Virol 79:10608–10618. https://doi.org/10.1128/JVI.79.16.10608-10618.2005.
23. Panaviene Z, Panavas T, Serva S, Nagy PD. 2004. Purification of the Cucumber necrosis virus replicase from yeast cells: role of coexpressed viral RNA in stimulation of replicase activity. J Virol 78:8254–8263. https://doi.org/10.1128/JVI.78.15.8254-8263.2004.
24. Panaviene Z, Baker JM, Nagy PD. 2003. The overlapping RNA-binding domains of p33 and p92 replicase proteins are essential for tombusvirus replication. Virology 308:191–205. https://doi.org/10.1016/s0042-6822(02)00132-0.
25. Oster SK, Wu B, White KA. 1998. Uncoupled expression of p33 and p92 permits amplification of tomato bushy stunt virus RNAs. J Virol 72:5845–5851. https://doi.org/10.1128/JVI.72.7.5845-5851.1998.
26. Scholthof KB, Scholthof HB, Jackson AO. 1995. The tomato bushy stunt virus replicase proteins are coordinately expressed and membrane associated. Virology 208:365–369. https://doi.org/10.1006/viro.1995.1162.
27. Serva S, Nagy PD. 2006. Proteomics analysis of the tombusvirus replicase: Hsp70 molecular chaperone is associated with the replicase and enhances viral RNA replication. J Virol 80:2162–2169. https://doi.org/10.1128/JVI.80.5.2162-2169.2006.
28. Nagy PD, Pogany J. 2006. Yeast as a model host to dissect functions of viral and host factors in tombusvirus replication. Virology 344:211–220. https://doi.org/10.1016/j.virol.2005.09.017.
29. Panavas T, Serviene E, Brasher J, Nagy PD. 2005. Yeast genome-wide screen reveals dissimilar sets of host genes affecting replication of RNA viruses. Proc Natl Acad Sci U S A 102:7326–7331. https://doi.org/10.1073/pnas.0502604102.
30. Rajendran KS, Nagy PD. 2006. Kinetics and functional studies on interaction between the replicase proteins of Tomato bushy stunt virus: requirement of p33:p92 interaction for replicase assembly. Virology 345:270–279. https://doi.org/10.1016/j.virol.2005.09.038.
31. Serviene E, Jiang Y, Cheng CP, Baker J, Nagy PD. 2006. Screening of the yeast yTHC collection identifies essential host factors affecting tombusvirus RNA recombination. J Virol 80:1231–1241. https://doi.org/10.1128/JVI.80.3.1231-1241.2006.
32. Serviene E, Shapka N, Cheng CP, Panavas T, Phuangrat B, Baker J, Nagy PD. 2005. Genome-wide screen identifies host genes affecting viral RNA recombination. Proc Natl Acad Sci U S A 102:10545–10550. https://doi.org/10.1073/pnas.0504844102.
33. Nagy PD, Pogany J. 2011. The dependence of viral RNA replication on co-opted host factors. Nat Rev Microbiol 10:137–149. https://doi.org/10.1038/nrmicro2692.

34. Nagy PD, Barajas D, Pogany J. 2012. Host factors with regulatory roles in tombusvirus replication. Curr Opin Virol 2:691–698. https://doi.org/10.1016/j.coviro.2012.10.004.
35. Nagy PD, Pogany J. 2010. Global genomics and proteomics approaches to identify host factors as targets to induce resistance against Tomato bushy stunt virus. Adv Virus Res 76:123–177. https://doi.org/10.1016/S0065-3527(10)76004-8.
36. Kovalev N, Pogany J, Nagy PD. 2020. Reconstitution of an RNA virus replicase in artificial giant unilamellar vesicles supports full replication and provides protection for the dsRNA replication intermediate. J Virol 94:e00267-20. https://doi.org/10.1128/JVI.00267-20.
37. Shah Nawaz-Ul-Rehman M, Martinez-Ochoa N, Pascal H, Sasvari Z, Herbst C, Xu K, Baker J, Sharma M, Herbst A, Nagy PD. 2012. Proteome-wide overexpression of host proteins for identification of factors affecting tombusvirus RNA replication: an inhibitory role of protein kinase C. J Virol 86:9384–9395. https://doi.org/10.1128/JVI.00019-12.
38. Mendu V, Chiu M, Barajas D, Li Z, Nagy PD. 2010. Cpr1 cyclophilin and Ess1 parvulin prolyl isomerases interact with the tombusvirus replication protein and inhibit viral replication in yeast model host. Virology 406:342–351. https://doi.org/10.1016/j.virol.2010.07.022.
39. Jiang Y, Serviene E, Gal J, Panavas T, Nagy PD. 2006. Identification of essential host factors affecting tombusvirus RNA replication based on the yeast Tet promoters Hughes Collection. J Virol 80:7394–7404. https://doi.org/10.1128/JVI.02686-05.
40. Sasvari Z, Alatriste Gonzalez P, Nagy PD. 2014. Tombusvirus-yeast interactions identify conserved cell-intrinsic viral restriction factors. Front Plant Sci 5:383. https://doi.org/10.3389/fpls.2014.00383.
41. Prasanth KR, Kovalev N, de Castro Martin IF, Baker J, Nagy PD. 2016. Screening a yeast library of temperature-sensitive mutants reveals a role for actin in tombusvirus RNA recombination. Virology 489:233–242. https://doi.org/10.1016/j.virol.2015.12.007.
42. Nawaz-Ul-Rehman MS, Prasanth KR, Xu K, Sasvari Z, Kovalev N, de Castro Martin IF, Barajas D, Risco C, Nagy PD. 2016. Viral replication protein inhibits cellular cofilin actin depolymerization factor to regulate the actin network and promote viral replicase assembly. PLoS Pathog 12:e1005440. https://doi.org/10.1371/journal.ppat.1005440.
43. Nawaz-Ul-Rehman MS, Reddisiva Prasanth K, Baker J, Nagy PD. 2013. Yeast screens for host factors in positive-strand RNA virus replication based on a library of temperature-sensitive mutants. Methods 59:207–216. https://doi.org/10.1016/j.ymeth.2012.11.001.
44. Li Z, Barajas D, Panavas T, Herbst DA, Nagy PD. 2008. Cdc34p ubiquitin-conjugating enzyme is a component of the tombusvirus replicase complex and ubiquitinates p33 replication protein. J Virol 82:6911–6926. https://doi.org/10.1128/JVI.00702-08.
45. Xu K, Nagy PD. 2015. RNA virus replication depends on enrichment of phosphatidylethanolamine at replication sites in subcellular membranes. Proc Natl Acad Sci U S A 112:E1782–E1791. https://doi.org/10.1073/pnas.1418971112.
46. Kovalev N, Nagy PD. 2013. Cyclophilin A binds to the viral RNA and replication proteins, resulting in inhibition of tombusviral replicase assembly. J Virol 87:13330–13342. https://doi.org/10.1128/JVI.02101-13.
47. Wang P, Heitman J. 2005. The cyclophilins. Genome Biol 6:226. https://doi.org/10.1186/gb-2005-6-7-226.
48. Arevalo-Rodriguez M, Wu X, Hanes SD, Heitman J. 2004. Prolyl isomerases in yeast. Front Biosci 9:2420–2446. https://doi.org/10.2741/1405.
49. Nagy PD, Wang RY, Pogany J, Hafren A, Makinen K. 2011. Emerging picture of host chaperone and cyclophilin roles in RNA virus replication. Virology 411:374–382. https://doi.org/10.1016/j.virol.2010.12.061.
50. Nagy PD. 2020. Host protein chaperones, RNA helicases and the ubiquitin network highlight the arms race for resources between tombusviruses and their hosts. Adv Virus Res 107:133–158. https://doi.org/10.1016/bs.aivir.2020.06.006.
51. Lin JY, Mendu V, Pogany J, Qin J, Nagy PD. 2012. The TPR domain in the host Cyp40-like cyclophilin binds to the viral replication protein and inhibits the assembly of the tombusviral replicase. PLoS Pathog 8:e1002491. https://doi.org/10.1371/journal.ppat.1002491.
52. Wu CY, Nagy PD. 2019. Blocking tombusvirus replication through the antiviral functions of DDX17-like RH30 DEAD-box helicase. PLoS Pathog 15:e1007771. https://doi.org/10.1371/journal.ppat.1007771.
53. Wu CY, Nagy PD. 2020. Role reversal of functional identity in host factors: dissecting features affecting pro-viral versus antiviral functions of cellular DEAD-box helicases in tombusvirus replication. PLoS Pathog 16:e1008990. https://doi.org/10.1371/journal.ppat.1008990.
54. Xu K, Nagy PD. 2016. Enrichment of phosphatidylethanolamine in viral replication compartments via co-opting the endosomal Rab5 small GTPase by a positive-strand RNA virus. PLoS Biol 14:e2000128. https://doi.org/10.1371/journal.pbio.2000128.
55. Li Z, Vizeacoumar FJ, Bahr S, Li J, Warringer J, Vizeacoumar FS, Min R, Vandersluis B, Bellay J, Devit M, Fleming JA, Stephens A, Haase J, Lin ZY, Baryshnikova A, Lu H, Yan Z, Jin K, Barker S, Datti A, Giaever G, Nislow C, Bulawa C, Myers CL, Costanzo M, Gingras AC, Zhang Z, Blomberg A, Bloom K, Andrews B, Boone C. 2011. Systematic exploration of essential yeast gene function with temperature-sensitive mutants. Nat Biotechnol 29:361–367. https://doi.org/10.1038/nbt.1832.
56. Young ME, Cooper JA, Bridgman PC. 2004. Yeast actin patches are networks of branched actin filaments. J Cell Biol 166:629–635. https://doi.org/10.1083/jcb.200404159.
57. Xu K, Huang TS, Nagy PD. 2012. Authentic in vitro replication of two tombusviruses in isolated mitochondrial and endoplasmic reticulum membranes. J Virol 86:12779–12794. https://doi.org/10.1128/JVI.00973-12.
58. Xu K, Lin JY, Nagy PD. 2014. The hop-like stress-induced protein 1 cochaperone is a novel cell-intrinsic restriction factor for mitochondrial tombusvirus replication. J Virol 88:9361–9378. https://doi.org/10.1128/JVI.00561-14.
59. Liu Y, Zhu W, Tan Y, Nakayasu ES, Staiger CJ, Luo Z-Q. 2017. A legionella effector disrupts host cytoskeletal structure by cleaving actin. PLoS Pathog 13:e1006186. https://doi.org/10.1371/journal.ppat.1006186.
60. Inaba JI, Xu K, Kovalev N, Ramanathan H, Roy CR, Lindenbach BD, Nagy PD. 2019. Screening Legionella effectors for antiviral effects reveals Rab1 GTPase as a proviral factor coopted for tombusvirus replication. Proc Natl Acad Sci U S A 116:21739–21747. https://doi.org/10.1073/pnas.1911108116.
61. Molho M, Lin W, Nagy PD. 2021. A novel viral strategy for host factor recruitment: the co-opted proteasomal Rpn11 protein interaction hub in cooperation with subverted actin filaments are targeted to deliver cytosolic host factors for viral replication. PLoS Pathog 17:e1009680. https://doi.org/10.1371/journal.ppat.1009680.
62. Cheng X, Deng P, Cui H, Wang A. 2015. Visualizing double-stranded RNA distribution and dynamics in living cells by dsRNA binding-dependent fluorescence complementation. Virology 485:439–451. https://doi.org/10.1016/j.virol.2015.08.023.
63. Bertrand E, Chartrand P, Schaefer M, Shenoy SM, Singer RH, Long RM. 1998. Localization of ASH1 mRNA particles in living yeast. Mol Cell 2:437–445. https://doi.org/10.1016/s1097-2765(00)80143-4.
64. Lin W, Liu Y, Molho M, Zhang S, Wang L, Xie L, Nagy PD. 2019. Co-opting the fermentation pathway for tombusvirus replication: compartmentalization of cellular metabolic pathways for rapid ATP generation. PLoS Pathog 15:e1008092. https://doi.org/10.1371/journal.ppat.1008092.
65. Barbosa Dos Santos I, Park SW. 2019. Versatility of cyclophilins in plant growth and survival: a case study in Arabidopsis. Biomolecules 9:20. https://doi.org/10.3390/biom9010020.
66. Kong G, Zhao Y, Jing M, Huang J, Yang J, Xia Y, Kong L, Ye W, Xiong Q, Qiao Y, Dong S, Ma W, Wang Y. 2015. The activation of Phytophthora effector Avr3b by plant cyclophilin is required for the nudix hydrolase activity of Avr3b. PLoS Pathog 11:e1005139. https://doi.org/10.1371/journal.ppat.1005139.
67. Trivedi DK, Yadav S, Vaid N, Tuteja N. 2012. Genome wide analysis of Cyclophilin gene family from rice and Arabidopsis and its comparison with yeast. Plant Signal Behav 7:1653–1666. https://doi.org/10.4161/psb.22306.
68. Franco IS, Shohdy N, Shuman HA. 2012. The Legionella pneumophila effector VipA is an actin nucleator that alters host cell organelle trafficking. PLoS Pathog 8:e1002546. https://doi.org/10.1371/journal.ppat.1002546.
69. Nagy PD. 2016. Tombusvirus-host interactions: co-opted evolutionarily conserved host factors take center court. Annu Rev Virol 3:491–515. https://doi.org/10.1146/annurev-virology-110615-042312.
70. Lappalainen P, Fedorov EV, Fedorov AA, Almo SC, Drubin DG. 1997. Essential functions and actin-binding surfaces of yeast cofilin revealed by systematic mutagenesis. EMBO J 16:5520–5530. https://doi.org/10.1093/emboj/16.18.5520.
71. Feng Z, Kovalev N, Nagy PD. 2020. Key interplay between the co-opted sorting nexin-BAR proteins and PI3P phosphoinositide in the formation of the tombusvirus replicase. PLoS Pathog 16:e1009120. https://doi.org/10.1371/journal.ppat.1009120.
72. Kovalev N, Inaba JI, Li Z, Nagy PD. 2017. The role of co-opted ESCRT proteins and lipid factors in protection of tombusviral double-stranded RNA replication intermediate against reconstituted RNAi in yeast. PLoS Pathog 13:e1006520. https://doi.org/10.1371/journal.ppat.1006520.

73. Marzook NB, Newsome TP. 2017. Viruses that exploit actin-based motility for their replication and spread. Handb Exp Pharmacol 235:237–261. https://doi.org/10.1007/164_2016_41.
74. Taylor MP, Koyuncu OO, Enquist LW. 2011. Subversion of the actin cytoskeleton during viral infection. Nat Rev Microbiol 9:427–439. https://doi.org/10.1038/nrmicro2574.
75. El Najjar F, Cifuentes-Munoz N, Chen J, Zhu H, Buchholz UJ, Moncman CL, Dutch RE. 2016. Human metapneumovirus induces reorganization of the actin cytoskeleton for direct cell-to-cell spread. PLoS Pathog 12:e1005922. https://doi.org/10.1371/journal.ppat.1005922.
76. Porter K, Day B. 2016. From filaments to function: the role of the plant actin cytoskeleton in pathogen perception, signaling and immunity. J Integr Plant Biol 58:299–311. https://doi.org/10.1111/jipb.12445.
77. Porter K, Day B. 2013. Actin branches out to link pathogen perception and host gene regulation. Plant Signal Behav 8:e23468. https://doi.org/10.4161/psb.23468.
78. Jelenska J, Kang Y, Greenberg JT. 2014. Plant pathogenic bacteria target the actin microfilament network involved in the trafficking of disease defense components. Bioarchitecture 4:149–153. https://doi.org/10.4161/19490992.2014.980662.
79. Shames SR, Liu L, Havey JC, Schofield WB, Goodman AL, Roy CR. 2017. Multiple Legionella pneumophila effector virulence phenotypes revealed through high-throughput analysis of targeted mutant libraries. Proc Natl Acad Sci U S A 114:E10446–E10454. https://doi.org/10.1073/pnas.1708553114.
80. Barajas D, Martin IFD, Pogany J, Risco C, Nagy PD. 2014. Noncanonical role for the host Vps4 AAA+ ATPase ESCRT protein in the formation of Tomato bushy stunt virus replicase. PLoS Pathog 10:e1004087. https://doi.org/10.1371/journal.ppat.1004087.
81. Foster G, Johansen E, Hong Y, Nagy PD. 2008. Plant virology protocols from viral sequence to protein function. Springer, New York, NY.
82. Barajas D, Xu K, de Castro Martin IF, Sasvari Z, Brandizzi F, Risco C, Nagy PD. 2014. Co-opted oxysterol-binding ORP and VAP proteins channel sterols to RNA virus replication sites via membrane contact sites. PLoS Pathog 10:e1004388. https://doi.org/10.1371/journal.ppat.1004388.
83. Chuang C, Prasanth KR, Nagy PD. 2017. The glycolytic pyruvate kinase is recruited directly into the viral replicase complex to generate ATP for RNA synthesis. Cell Host Microbe 22:639–652. https://doi.org/10.1016/j.chom.2017.10.004.